

Quantified H I Morphology VII: The Morphology of Extended Disks in UV and H I

B. W. Holwerda^{1*}, N. Pirzkal,² and J. S. Heiner³

¹ *European Space Agency, ESTEC, Keplerlaan 1, 2200 AG, Noordwijk, the Netherlands*

² *Space Telescope Science Institute, Baltimore, MD 21218, USA*

³ *Centro de Radioastronomía y Astrofísica, Universidad Nacional Autónoma de México, 58190 Morelia, Michoacán, Mexico*

Accepted 1988 December 15. Received 1988 December 14; in original form 1988 October 11

ABSTRACT

Extended UltraViolet (XUV) disks have been found in a substantial fraction of late-type –S0, spiral and irregular– galaxies. Similarly, most late-type spirals have an extended gas disk, observable in the 21cm radio line (H I). The morphology of galaxies can be quantified well using a series of scale-invariant parameters; Concentration-Asymmetry-Smoothness (CAS), Gini, M_{20} , and G_M parameters. In this series of papers, we apply these to H I column density maps to identify mergers and interactions, lopsidedness and now XUV disks.

In this paper, we compare the quantified morphology and effective radius (R_{50}) of the Westerbork observations of neutral Hydrogen in Irregular and Spiral galaxies Project (*WHISP*) H I maps to those of far-and near-ultraviolet images obtained with GALEX, to explore how close the morphology and scales of H I and UV in these disks correlate. We find that XUV disks do not stand out by their effective radii in UV or H I. However, the concentration index in FUV appears to select some XUV disks. And known XUV disks can be identified via a criterion using Asymmetry and M_{20} ; 80% of XUV disks are included but with 55% contamination. This translates into 61 candidate XUV disk out of our 266 galaxies, –23%– consistent with previous findings. Otherwise, the UV and H I morphology parameters do not appear closely related.

Our motivation is to identify XUV disks and their origin. We consider three scenarios; tidal features from major mergers, the typical extended H I disk is a photo-dissociation product of the XUV regions and both H I and UV features originate in cold flows fueling the main galaxy.

We define extended H I and UV disks based on their concentration ($C_{HI} > 5$ and $C_{FUV} > 4$ respectively), but that these two subsamples never overlap in the *WHISP* sample. This appears to discount a simple photo-dissociation origin of the outer H I disk.

Previously, we identified the morphology space occupied by ongoing major mergers. Known XUV disks rarely reside in the merger dominated part of H I morphology space but those that do are Type 1. Exceptions, XUV disks in ongoing mergers, are the previously identified UGC 4862 and UGC 7081, 7651, and 7853. This suggests cold flows as the origin for the XUV complexes and their surrounding H I structures.

Key words:

1 INTRODUCTION

Interest in the outskirts of spiral galaxy disks has increased over recent years as these regions are the site of the most recent acquisition of gas for these systems (e.g. Sancisi et al.

2008), as well as low-level star-formation (e.g., Dong et al. 2008; Bigiel et al. 2010a; Alberts et al. 2011, for recent results), making these faint outskirts the interface between the island universes –the galaxies themselves– and the cosmic web of primordial gas.

The low-level star-formation was first discovered in H α emission by Ferguson et al. (1998) and Lelièvre &

* E-mail: benne.holwerda@esa.int

Roy (2000). After the launch of the Galaxy Evolution Explorer (GALEX, Martin et al. 2005), initial anecdotal evidence pointed to ultraviolet disks of spiral galaxies extending much beyond their optical radius (Thilker et al. 2005b,a; Gil de Paz et al. 2005, 2007b; Zaritsky & Christlein 2007). Subsequent structural searches for these Extended Ultraviolet (XUV) Disks by Thilker et al. (2007) and Lemonias et al. (2011) find that some 20–30% of spirals possess an XUV disk and 40% of S0s (Moffett et al. 2011), making this type of disk common but not typical for spiral and S0 galaxies. These XUV disk complexes are generally ~ 100 Myr old, explaining why most lack H α (Alberts et al. 2011), as opposed to a top-light IMF (as proposed by Meurer et al. 2009), and sub-solar but not excessively low metallicities (Gil de Paz et al. 2007b; Bresolin et al. 2009; Werk et al. 2010, $0.1 - 1 Z_{\odot}$, based on emission lines). Additionally, it has been known for some time now that atomic hydrogen (H I) as observed by the 21cm fine structure line also extends well beyond the optical disk of spiral galaxies (e.g., Begeman 1989; Meurer et al. 1996, 1998; Swaters et al. 2002a; Noordermeer et al. 2005a; Walter et al. 2008; Boomsma et al. 2008; Elson et al. 2011; Heald et al. 2011b,a; Zschaechner et al. 2011). In those few cases where both high-quality H I and deep GALEX data are available, a close relation in their respective morphology was remarked upon (Bigiel et al. 2010a). While we have to wait for the all-sky surveys in H I to catch up to the coverage of the GALEX surveys (e.g., the wide survey with WSRT/APERTIF or the WALLABY survey with ASKAP), we can compare the morphology for those galaxies for which uniform H I information is available.

The canonical view of the origin of the XUV disks, is that the Kennicutt-Schmidt law (Kennicutt 1998) needs to be extended to low global surface densities of gas and the formation of individual O-stars in the very outskirts of disks (Cuillandre et al. 2001; Bigiel et al. 2010b). The recent accretion of cold gas flows (Kereš et al. 2005) into the H I disk is the origin for the young stars (the fueling rate implied by XUV disks is explored in Lemonias et al. 2011) and H I warps (Roškar et al. 2010). The fraction of spirals that have an XUV disk ($\sim 20 - 30\%$) supports this scenario as the remaining spirals may simply have no current cool gas inflow. In this case, one would expect UV and H I morphology to follow each other reasonably closely for the XUV disks but not for many of the others, as the star-formation in the inner disk is more closely related to the molecular phase (Bigiel et al. 2008). However, the existence of XUV disks pose an intriguing alternate possibility for the origin of the atomic hydrogen disk. Instead of primordial gas accreting onto the disk, the H I disk could also be the byproduct of photodissociation of molecular hydrogen on the ‘skins’ of molecular clouds by the ultraviolet flux of the young stars in the XUV disk (see Allen et al. 1997; Allen 2002; Allen et al. 2004). This explanation has been explored in the stellar disks of several nearby galaxies (Heiner et al. 2008a,b, 2009, 2010). Gil de Paz et al. (2007b) calculate the time-scales (molecular gas dissociation and re-formation) involved but these are inconclusive regarding the origin of the XUV disk. In this scenario, one would expect the UV and H I morphologies to follow each other closely in all cases; in the outer disk, the UV flux from a few young stars would reach out to large areas of the low-column density gas to dissociate enough hydrogen to form the outer H I disk. Thus, the low-flux and

low H I column density morphology –those defining the limits and extent of the XUV and H I disks– should show a close relation in parameters such as concentration, Gini, M_{20} and the effective radius. A third explanation is in terms of recent tidal interaction. A major merger often pulls gas out of the planes of galaxies and triggers star-forming events. Some anecdotal evidence (e.g., UGC 04862 is a late-stage major merger Torres-Flores et al. 2012) does point to this possible origin. In this scenario, one would expect that most H I disks hosting an XUV disk would be seriously tidally disrupted.

In this series of papers, we have explored the quantified morphology of available H I maps with the common parameters for visible morphology; concentration-asymmetry-smoothness, Gini and M_{20} and G_M . In Holwerda et al. (2011c), we compare the H I morphology to other wavelengths, noting that the H I and ultraviolet morphologies are closely related. In subsequent papers of the series, we use the H I morphology to identify mergers (Holwerda et al. 2011d), their visibility time (Holwerda et al. 2011a) and subsequently infer a merger rate from *WHISP* (Holwerda et al. 2011b) as well as identify phenomena unique to cluster members (Holwerda et al. 2011e).

In this paper, we explore the morphological link between the H I and XUV disks in the Westerbork H I Survey Project (*WHISP*, van der Hulst et al. 2001; van der Hulst 2002), a survey of several hundred H I observations of nearby galaxies. We complement this data with GALEX images to explore the morphology and typical scales of these maps. A direct and quantified comparison between the gas and ongoing star-formation morphology could help answer open questions regarding the origin and nature of XUV disks: how do their respective sizes relate? Are their morphologies closely related in every case? Do their respective morphologies point to a dominant formation mechanism; gas accretion, photodissociation or tidal? Are XUV disks in morphologically distinct or typical H I disks? Are XUV disks embedded in H I disks that appear to be in an active interaction? What is the relation between UV flux and H I column density in the XUV disks, especially the outer disk?

The paper is organized as follows; §2 gives the definitions of the quantified morphology parameters we employ, and §3 describes the origin the data. We describe the application of the morphological parameters and the results in §4 and 5, and we discuss them in §6. We list our conclusions and discuss possible future work in §7.

2 MORPHOLOGICAL PARAMETERS

In this series of papers, we use the Concentration-Asymmetry-Smoothness parameters (CAS, Conselice 2003), combined with the Gini- M_{20} parameters from Lotz et al. (2004) and one addition of our own G_M . We have discussed the definitions of these parameters in the previous papers, as well as how we estimate uncertainties for each. Here, we will give a brief overview but for details we refer the reader to Holwerda et al. (2011c,d).

We select pixels in an image as belonging to the galaxy based on the outer H I contour and adopt the position from the 2MASS catalog (Kleinmann et al. 1994) as the central position of the galaxy. Given a set of n pixels in each object, iterating over pixel i with value I_i , position x_i, y_i with the

centre of the object at x_c, y_c these parameters are defined as:

$$C = 5 \log(r_{80}/r_{20}), \quad (1)$$

with r_f as the radial aperture, centered on x_c, y_c containing percentage f of the light of the galaxy (see definitions of r_f in Bertin & Arnouts 1996; Holwerda 2005).¹ We include the r_{50} , or “effective radius” in our catalog as well.

$$A = \frac{\sum_i |I_i - I_{180}|}{\sum_i |I(i)|}, \quad (2)$$

where I_{180} is the pixel at position i in the galaxy’s image, after it was rotated 180° around the centre of the galaxy.

$$S = \frac{\sum_{i,j} |I(i,j) - I_S(i,j)|}{\sum_{i,j} |I(i,j)|}, \quad (3)$$

where I_S is pixel i in a smoothed image. The type of smoothing (e.g., boxcar or Gaussian) has changed over the years. We chose a fixed 5” Gaussian smoothing kernel for simplicity.

The Gini coefficient is defined as:

$$G = \frac{1}{\bar{I}n(n-1)} \sum_i (2i - n - 1)I_i, \quad (4)$$

where the list of n pixels was first ordered according to value and \bar{I} is the mean pixel value in the image.

$$M_{20} = \log\left(\frac{\sum_i M_i}{M_{tot}}\right), \text{ for } \sum_i I_i < 0.2I_{tot}, \quad (5)$$

where M_i is the second order moment of pixel i ; $M_i = I_i \times [(x - x_c)^2 + (y - y_c)^2]$. M_{tot} is the second order moment summed over all pixels in the object and M_{20} is the relative contribution of the brightest 20% of the pixels in the object. Instead of using the intensity of pixel i , the Gini parameter can be defined using the second order moment:

$$G_M = \frac{1}{\bar{M}n(n-1)} \sum_i (2i - n - 1)M_i, \quad (6)$$

These parameters trace different structural characteristics of a galaxy’s image but these do not span an orthogonal parameter space (see also the discussion in Scarlata et al. 2007).

3 DATA

We use three data sets for this paper; H I radio observations from *WHISP* or *THINGS*, and ultraviolet observations from GALEX space telescope observations.

3.1 WHISP Sample

The starting dataset here is the 266 observations done as part of the Westerbork observations of neutral Hydrogen in Irregular and SPiral galaxies (*WHISP*, van der Hulst et al. 2001; van der Hulst 2002, ; 339 individual galaxies) that also have reasonable quality FUV and NUV data. The *WHISP*

observation targets were selected from the Uppsala General Catalogue of Galaxies (Nilson 1973), with blue major axis diameters $> 2'.0$, declination (B1950) > 20 degrees and flux densities at 21-cm larger than 100 mJy, later lowered to 20 mJy. Observation times were typically 12 hours of integration. The galaxies satisfying these selection criteria generally have redshifts less than 20000 km/s ($z < 0.07$). *WHISP* has mapped the distribution and velocity structure of H I in several hundreds of nearby galaxies, increasing the number of H I observations of galaxies by an order of magnitude. The *WHISP* project provides a uniform database of data-cubes, zeroth-order and velocity maps. Its focus has been on the structure of the dark matter halo as a function of Hubble type, the Tully-Fisher relation and the dark matter content of dwarf galaxies (Swaters et al. 2002b; Swaters & Balcells 2002; Noordermeer et al. 2005b; Zwaan et al. 2005). Until the large all-sky surveys with new instruments are completed, *WHISP* is the largest, publicly available data-set of resolved H I observations². We compiled a catalogue of basic data (position, radial velocity etc.) (see for details Holwerda et al. 2011b).

3.1.1 H I Data

We use the highest available resolution zero-moment maps (beam size of $\sim 12'' \times 12''/\sin(\delta)$), from the WOW website and converted these to M_\odot/pc^2 column density maps with J2000 coordinates and of the same size as the GALEX postage stamp (see for details Holwerda et al. 2011b).

3.1.2 GALEX data

To complement the H I column density maps, we retrieved GALEX (Martin et al. 2005) postage stamps from <http://skyview.gsfc.nasa.gov>, near- and far-ultraviolet (1350–1750 and 1750–2750 Å). The majority of observations were taken as part of the AIS, MIS, NGS, etc. imaging surveys and hence vary in depth and signal-to-noise. Spatial resolution is 4–6”, depending on position in the field-of-view.

Of the 339 galaxies in *WHISP*, 266 had reliable FUV information and this cross-section is what we use for the remainder of the paper. The FUV images with H I contours overlaid are shown in Figures 1, 2, and Figures ?? ?? and all galaxies in appendix C (*electronic edition*).

3.1.3 XUV classifications

In the *WHISP* sample, Thilker et al. (2007) classified 22 galaxies for the presence and type of XUV disks. The Type 1 XUV disks are characterized by discrete regions out to high radii and Type 2 by an anomalously large, UV-bright outer zone of low optical surface brightness. Table 1 lists the XUV classifications for the *WHISP* sample; 22 from Thilker et al. (2007) and a single one from Lemonias et al. (2011). The latter study’s lack of overlap is unsurprising as they focus on a more distant sample in complement to the Thilker et al.’s nearby sample ($D < 40\text{Mpc}$). We designate an XUV disk with both a Type 1 and Type 2 as Type 1/2 to discriminate in

¹ We must note that the earlier version of our code contained an error, artificially inflating the concentration values. A check revealed this to be $C_{new} = 0.38C_{old}$, and we adopt the new, correct values in this paper.

² Available at “Westerbork On the Web” (WOW) project at AS-TRON (<http://www.astron.nl/wow/>).

the plots below and mark those galaxies in *WHISP* surveyed by Thilker et al. that do not have an XUV disk as Type 0.

Figures 1 and 2 show the overlap between *WHISP* and the XUV disks identified by Thilker. The Type 1 collection includes a single merger remnant (UGC 4862) and some H I disks that appear slightly lopsided, tentatively supporting a tidal origin as one path to generate Type 1 disks. Figure 3 shows the H I contours around those *WHISP* galaxies inspected by Thilker et al. but not found to contain an XUV disk. There are two instances of clear ongoing mergers as well as a variety of H I morphologies.

3.2 THINGS

Since there overlap between *WHISP* sample and the Thilker et al XUV classification sample is small, we also compare the *THINGS* survey's H I and FUV morphologies to their classifications of XUV disks (Table 2). We use the morphological information from Holwerda et al. (2011c), with the concentration definition appropriately amended. The morphological classifications are based on the public datasets from the H I Nearby Galaxy Survey (*THINGS*, Walter et al. 2008)³, and GALEX Nearby Galaxy Atlas (NGA, Gil de Paz et al. 2007a)⁴, retrieved from MAST (<http://galex.stsci.edu>). We use the robust-weighted (RO) *THINGS* column density maps as these are similar in resolution as the native resolution of GALEX for the contour of $0.3 \times 10^{20} \text{ cm}^{-2}$, approximately the spatial extent of the H I disk. Table 2 lists the *THINGS* galaxies that have XUV disk classifications from Thilker et al. (2007). The benefits of the *THINGS* sample are that there is an XUV classification for all galaxies, the H I and UV data are of comparable spatial resolution, and the GALEX observations are of uniform depth. Drawbacks are that is is an equally small sample as the *WHISP* overlap and there is only a single ongoing merger in this sample as it was constructed to be quiescent.

4 APPLICATION OF QUANTIFIED MORPHOLOGY TO H I AND GALEX DATA

Before we compute the quantified morphology parameters described above, we preprocess the images as follows. First, we cut out a postage stamp of both the H I maps and GALEX data centered on the UGC position. Similar to Holwerda et al. (2011b), we use a stamp size of 22×22 arcmin around this position. We then smooth the GALEX data to approximately the same spatial resolution as the *WHISP* H I data ($\sim 12''$). We use the H I map to define the part of the data over which the morphological parameters are computed over in the same manner as in Holwerda et al. (2011d,b); a threshold of $10^{20} \text{ atoms/cm}^2$.

We then compute the above quantified morphology parameters for the H I map and far-, and near-ultraviolet images (summarized in Tables ??, ?? and ??, *full versions in the electronic edition*). In addition to the above parameters, we compute the effective or half-light radius (R_{50}) for each image as an indication of disk size on the sky.

Table 1. XUV disks classified by Thilker et al. (2007) and one from Lemonias et al. (2011) for the *WHISP* galaxies in their respective samples.

| Name | UGC | Type |
|----------|-------|------|
| - | 1913 | 0 |
| - | 4165 | 0 |
| - | 4274 | 0 |
| - | 4273 | 0 |
| NGC 2541 | 4284 | 2 |
| - | 4325 | 0 |
| - | 4499 | 0 |
| NGC 2782 | 4862 | 1 |
| - | 5556 | 0 |
| NGC 3319 | 5789 | 2 |
| NGC 3344 | 5840 | 1 |
| - | 6856 | 0 |
| - | 7323 | 0 |
| NGC 4258 | 7353 | 1 |
| - | 7651 | 0 |
| NGC 4559 | 7766 | 1 |
| - | 7853 | 0 |
| NGC 4625 | 7861 | 1 |
| NGC 5832 | 9649 | 1/2 |
| - | 10445 | 1/2 |
| - | 10791 | 1 |
| - | 12754 | 0 |

Table 2. XUV disks classified by Thilker et al. (2007) for those *THINGS* galaxies in their sample.

| Name | Type | Reference |
|-------------|------|------------------------------|
| NGC 628 | 1 | Lelièvre & Roy (2000) |
| NGC 925 | 0 | Alberts et al. (2011) |
| NGC 2403 | 1/2 | |
| Holmberg-II | 0 | |
| M81A | 0 | |
| DDO53 | 0 | |
| NGC 2841 | 1 | Alberts et al. (2011) |
| NGC 2903 | 0 | |
| HolmbergI | 0 | |
| NGC 2976 | 0 | |
| NGC 3031 | 1 | |
| NGC 3184 | 0 | |
| NGC 3198 | 1 | |
| IC2574 | 2 | |
| NGC 3351 | 0 | |
| NGC 3521 | 0 | |
| NGC 3621 | 1 | Alberts et al. (2011) |
| NGC 3627 | 0 | |
| NGC 4736 | 0 | Zaritsky & Christlein (2007) |
| DDO154 | 0 | |
| NGC 4826 | 0 | |
| NGC 5055 | 1 | Alberts et al. (2011) |
| NGC 5194 | 0 | |
| NGC 5457 | 1 | |
| NGC 6946 | 0 | |
| NGC 7331 | 0 | |
| NGC 7793 | 0 | |

³ <http://www.mpia-hd.mpg.de/THINGS/>

⁴ <http://galex.stsci.edu/GR4/>

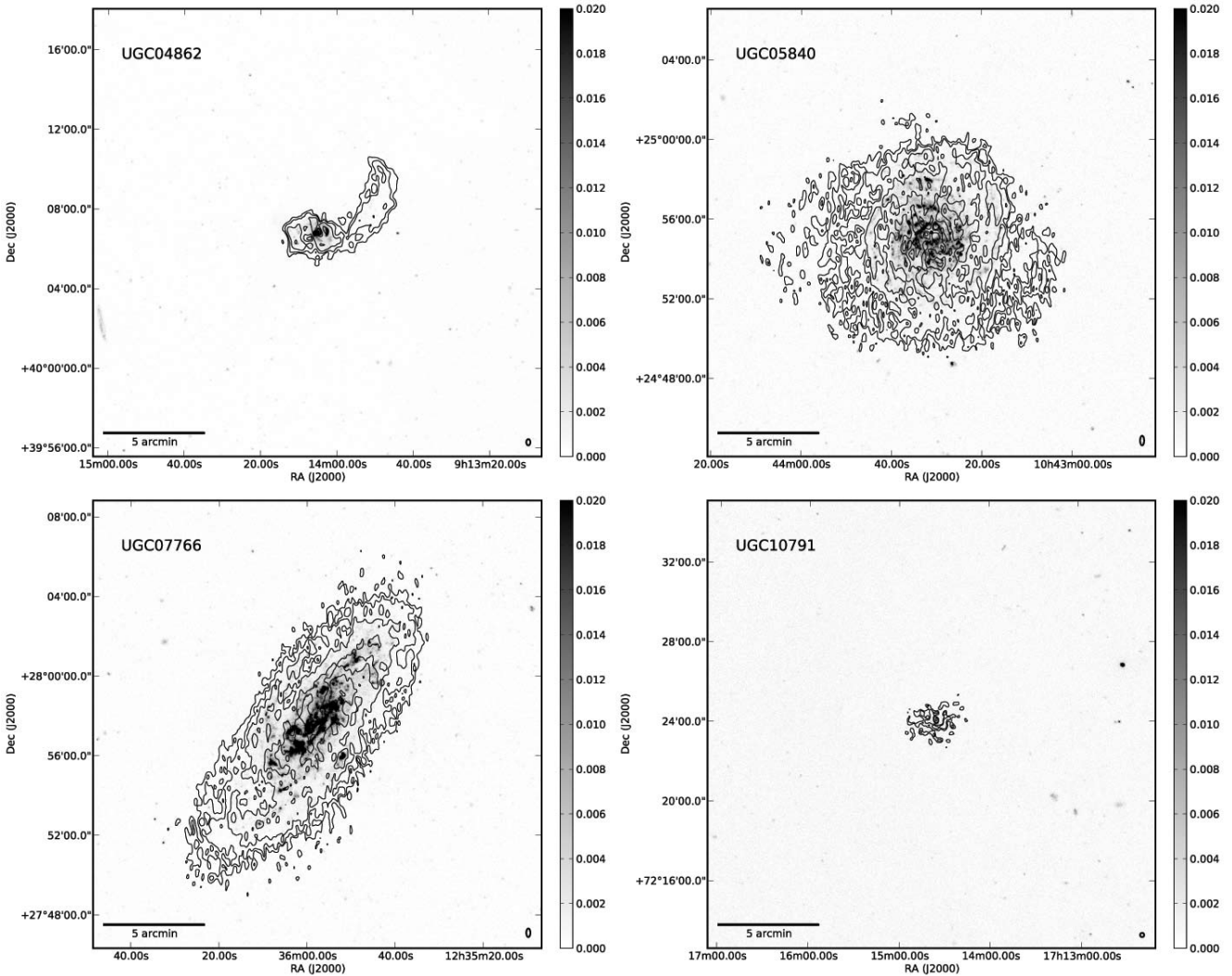


Figure 1. The few examples of xUV disks, Type 1 (individual UV complexes) as classified by Thilker et al. (2007) with complementary H I data in *WHISP*. The tidal feature in UGC 04862 is studied in detail by Torres-Flores et al. (2012), who report high metallicities and 1-11 Myr ages for the UV complexes. They speculate that their origin is either from the galaxies that formed UGC 04862 or that the current star-formation is a later generation, enriched system.

5 ANALYSIS

To explore in what type of H I disk xUV disks predominantly occur, we first compare the relative effective radii of the H I and UV disks, secondly compare the individual morphological parameters in both H I and UV against one another, and thirdly explore the UV and H I morphologies alone, to explore if xUV can be identified from UV morphology and to see if xUV disks are predominantly in merging or interacting disks.

5.1 Effective Radii

First we compare the relative sizes of the NUV and FUV disks and the H I disk through their effective radii, the radius which contains 50% of the total flux. A naive expectation would be that in the case of extended UV disks, these would be similar to the H I values. Figure 4 shows the ratio of the effective radii (R_{eff}) for H I and FUV or NUV. Nei-

ther ratio singles out those identified by Thilker et al. (2007) as extended UV disks. Thus the ratio of effective radii is not a good metric to automatically select xUV disks.

5.2 UV vs H I Morphologies

Figures 5 and 6 show the Concentration, Asymmetry, Smoothness, Gini, M_{20} and the G_M of the NUV and FUV compared to their values in the H I maps, as computed over the same area and convolved to the same spatial resolution. We note that our approach is different from that of Lemonias et al. (2011) who use the *optical* concentration to identify the approximate galaxy type.

Concentration of the UV and the H I shows two distinct sets of outliers. One where the UV concentration is more than three; these are relatively extended disks. Some of the xUV disks from Thilker et al. (2007) can be found here, but by no means all; two type 1/2 and one type 1 is not. However, six of the non-xUV disks are also above the

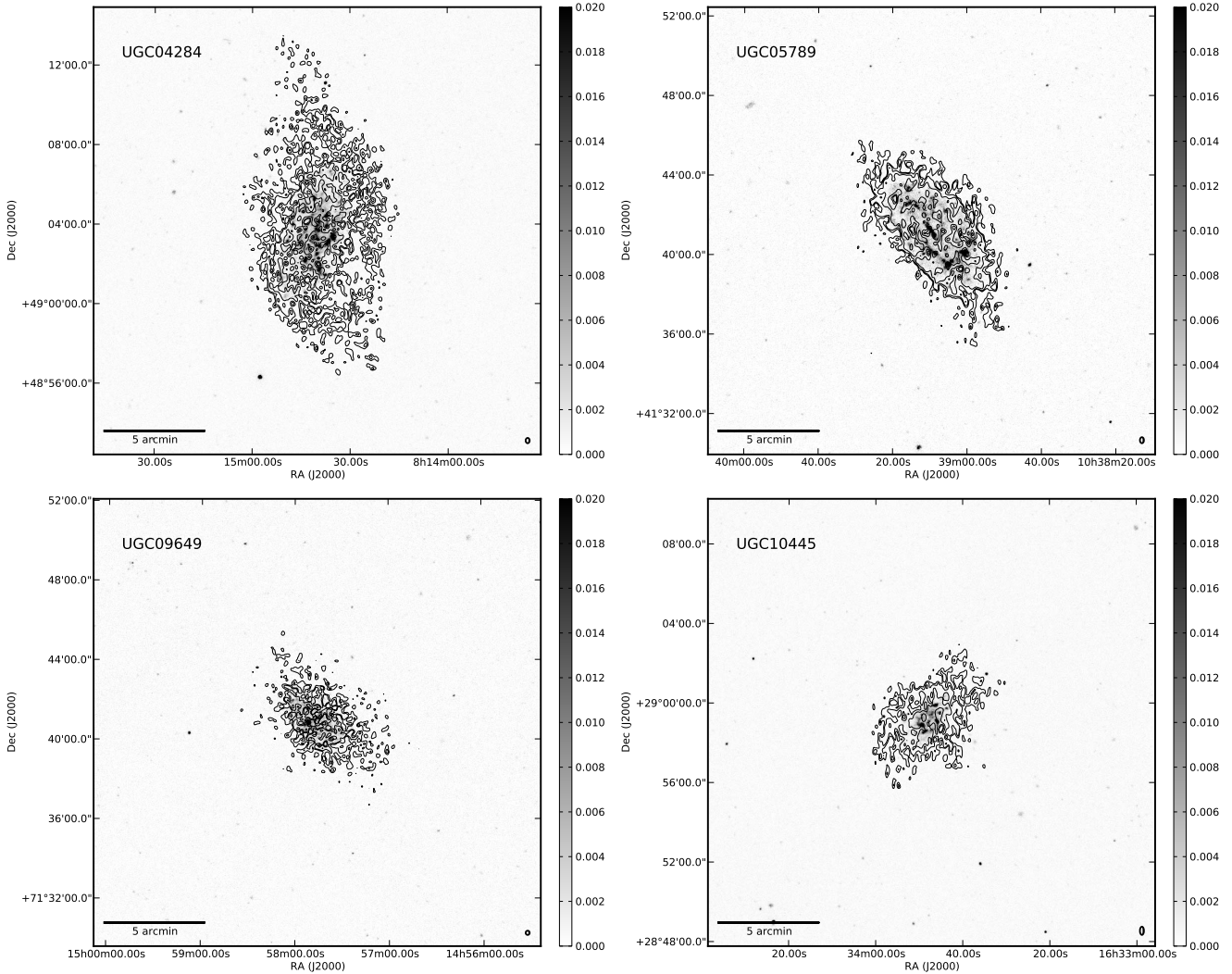


Figure 2. The two known examples of Type 2 XUV disks, a ring of UV outside the optical disk (top) and the two examples of Type 1/2, a combination of Types 1 and 2, as classified by Thilker et al. (2007), which are also in the *WHISP* sample. The H I morphology is remarkably flocculant and lacks grand spiral structure.

$C_{FUV} > 4$ line. Figures 7 and 8 show that most Type 1 in the *THINGS* sample are here. The second set of outliers have H I concentration indices exceeding $C_{HI} > 5$. However, these are not necessarily the classical H I disks which extend well outside the stellar disk. High concentration values such as these often indicate recent tidal activity (Holwerda et al. 2011d). We will use the Concentration indices in FUV and H I to set our own supplementary definition of an extended disk; XUV_c disks are defined by $C_{FUV} > 4$ and extended H I disks (XH I) by $C_{HI} > 5$ in the other plots. We do so to identify these outliers in the other plots to explore their nature, not to supplant the original detailed classification by Thilker et. al. The XUV_c disks have UV flux distributed throughout their otherwise unremarkable H I disk and XH I disks are extended in H I but not special in UV. If we compare the ratio of concentration indices in Figure 9 for the *WHISP* galaxies, both the XUV_c and XH I disks –unsurprisingly– stand out very clearly. This is confirmed by the ratios of *THINGS* concentration index in Figure 10. We note, however, that if one applies these criteria blindly to the *THINGS* data (dashed

lines in Figure 8), one would conclude that most *THINGS* galaxies are XUV_c disks. Morphological criteria such as these need to be recalibrated when applied to different quality data.

XUV and XUV_c disks have much lower values of the M_{20} parameter in the UV than the general *WHISP* population. There is a general trend between M_{20} and concentration (specifically for the 3.6 μ m Spitzer images Muñoz-Mateos et al. 2009, Holwerda et al. *in preparation*), so extreme values for this parameter are not surprising as such, especially if identified with a concentration criterion (see also Figure 11). The *lower* value of M_{20} implies that regions that make up the XUV disk do not contribute to the brightest 20% of all the pixels in these UV images.; the general UV flux is more extended and hence the second order moment is less concentrated in the brightest few regions. The H I M_{20} values however are quite within the normal range of *WHISP* galaxies. Thus, perhaps the UV M_{20} values offer an alternative automated definition of XUV disks in combination with concentration.

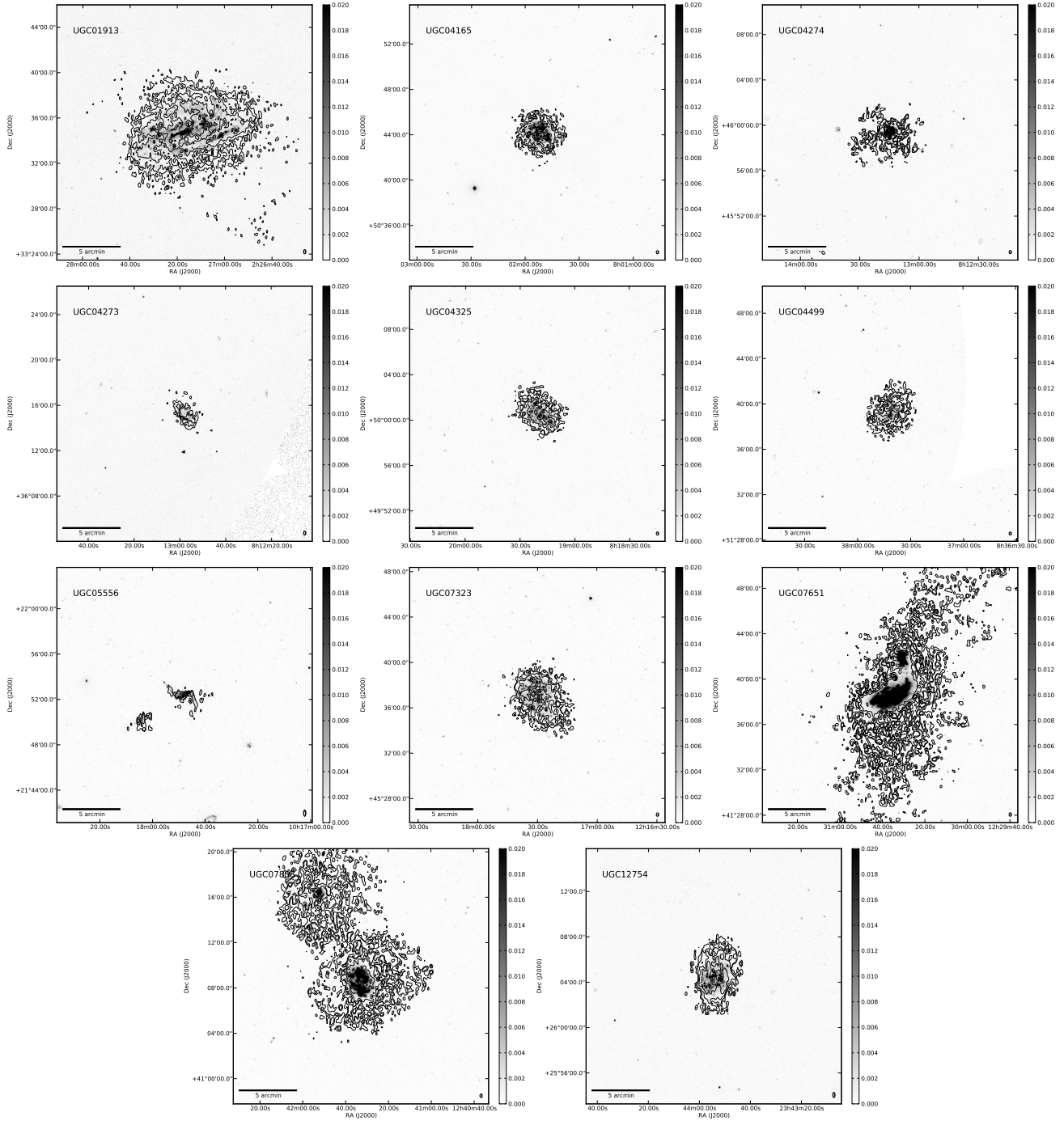


Figure 3. The Type 0 XUV disks –no XUV disk identified by Thilker et al. (2007)– in the *WHISP* sample. There are two ongoing major mergers as well as a range of H I morphologies.

The XUV disks show a median value for Asymmetry in FUV, but the full range in H I.

In UV smoothness, the XUV disks do not stand well apart from the general *WHISP* population. In the case of the G and G_M parameters, XUV disks avoid extreme values for the UV and generally fall below the $G_M(\text{H I}) = 0.6$ criterion for interactions. In the case of most of the H I morphological parameters, the values for the XUV disks are typical for the bulk of *WHISP* galaxies.

Based on their relative H I and UV morphologies, the previously identified or automatically identified XUV disks mostly stand out in their UV concentration and M_{20} values. In the remaining UV parameters and all H I morphological values, they appear to be mixed in with the bulk of the *WHISP* (Figures 5 and 6) and *THINGS* (Figures 7 and 8).

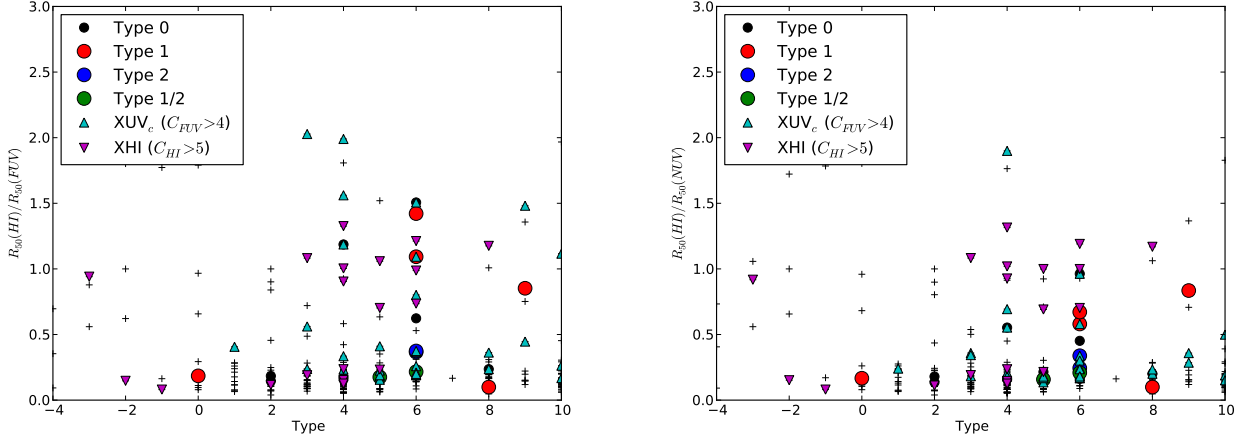


Figure 4. The ratio of effective radii (R_{50}) of the H I over UV as a function of Hubble type as a function of type.

Table 3. XUV disk selection criteria and their success (percentage of all bona-fide XUV disks included) and contamination rate (percentage of included objects that are non-XUV):

| Criterion | WHISP | | | THINGS | | |
|---|---------|----------|-----|---------|----------|--|
| | XUV (%) | Cont (%) | Nr | XUV (%) | Cont (%) | |
| $C_{FUV} > 4$ | 30. | 57 | 31 | 25 | 71 | |
| $ A - (-0.26667 * M_{20}) + 0.12 < 0.14$ | 80 | 55 | 109 | - | - | |
| $ A - (-0.26667 * M_{20}) + 0.12 < 0.14$ | - | - | - | 87 | 56 | |

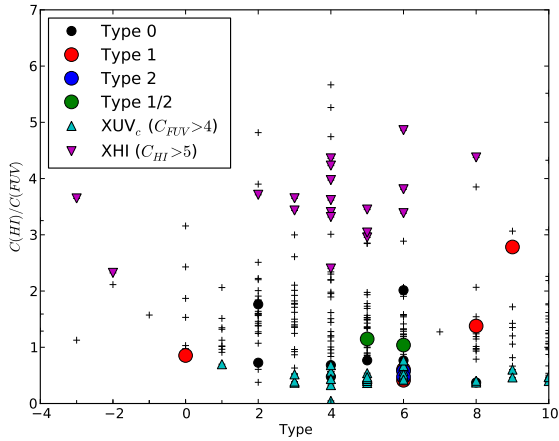


Figure 9. The ratio of Concentration in H I over that in UV as a function of Hubble type. In this case (as expected), the XUV and XHI disks stand out.

5.3 XUV disk UV morphology

In this section we look at the UV morphological parameters in detail to explore if bona-fide XUV disks can be identified from their UV morphology alone – as computed over an area defined by the H I disk. For this we can use the 22 galaxies in *WHISP* and the *THINGS* sample, both classified by Thilker et al.

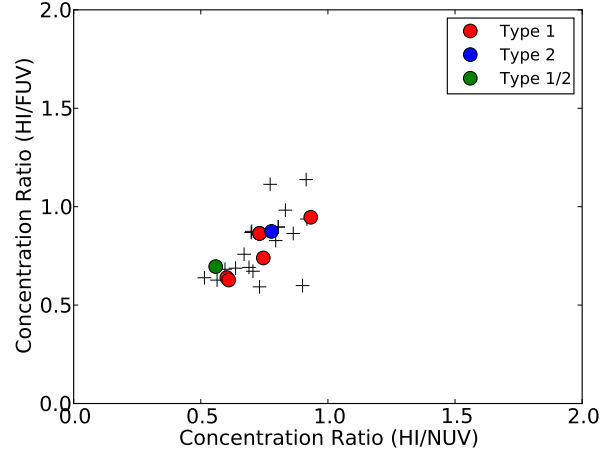


Figure 10. The ratio of concentration of the H I over UV (NUV and FUV) for the *THINGS* galaxies

Figure 11 shows the FUV parameters for the XUV disks identified by Thilker et al. (2007) as well as those disks inspected but without an extended UV component for both samples.

The above Concentration-only criterion ($XUV_c, C_{FUV} > 4$) pre-selects a number of the XUV disks but it would miss several bona-fide XUV disks as well as include many false positives. Using the information in two (or possibly more)

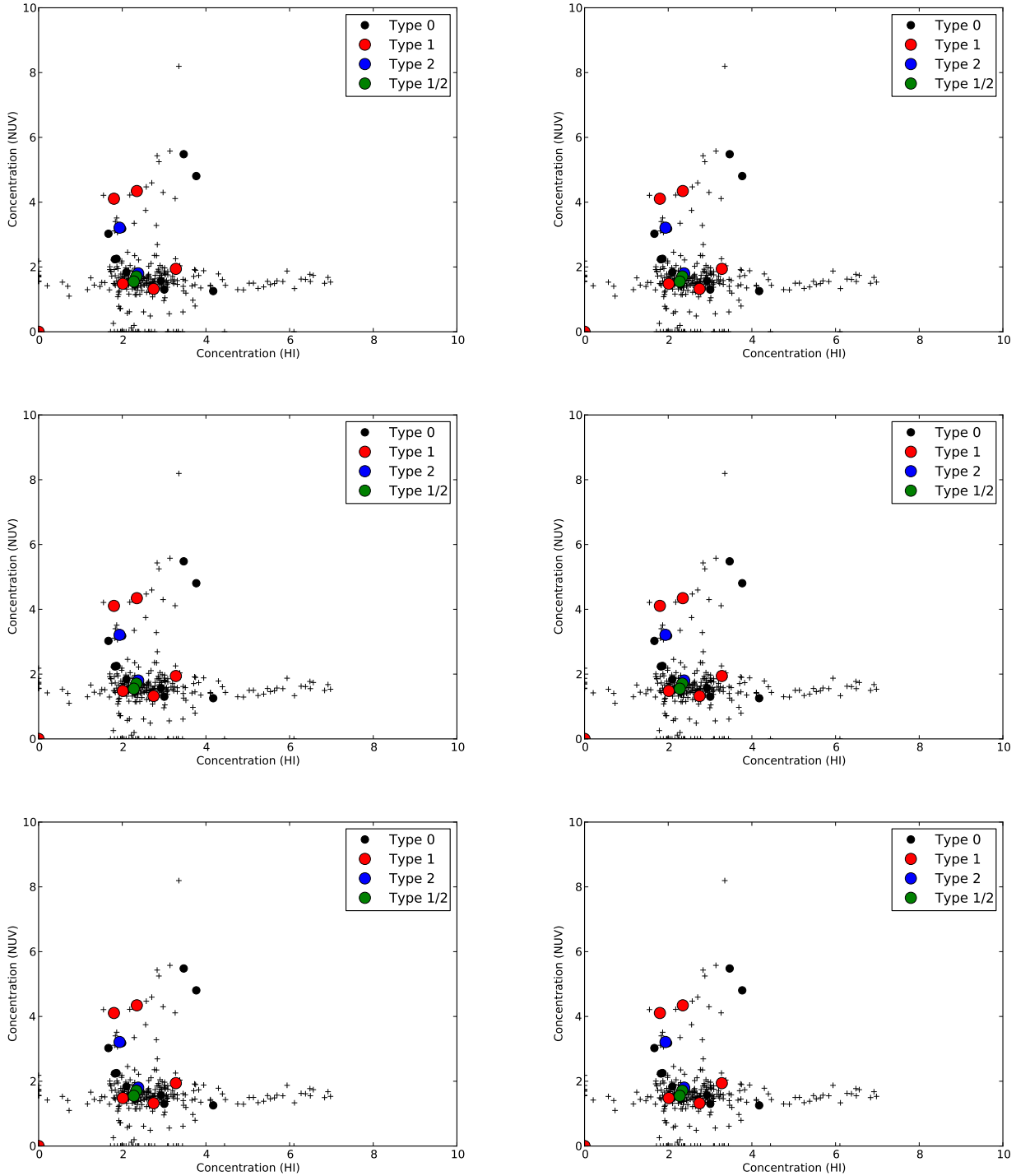


Figure 5. The morphological parameters of the H I disk and NUV data; concentration (C), asymmetry (A), smoothness (S), the Gini index (G), and the second order moment of the brightest 20% of the pixels (M_{20}), and the gini index of the second order moment (G_M).

parameters is how we identify mergers and may identify (candidate) XUV disks. On inspection of the distributions of the NUV and FUV parameters (Figures ?? and ??), there are several combinations of parameters that offer the possibility of pre-selecting XUV disks without too much loss: Gini-Asymmetry, M_{20} -Asymmetry and Gini- G_M . The goal

is not to just select only the bona-fide, previously identified XUV disks but also to exclude as many disks, that were previously classified as non-XUV as practical. This latter criterion immediately excludes Gini-Asymmetry and Gini- G_M combinations. The combination of M_{20} and Asymmetry in

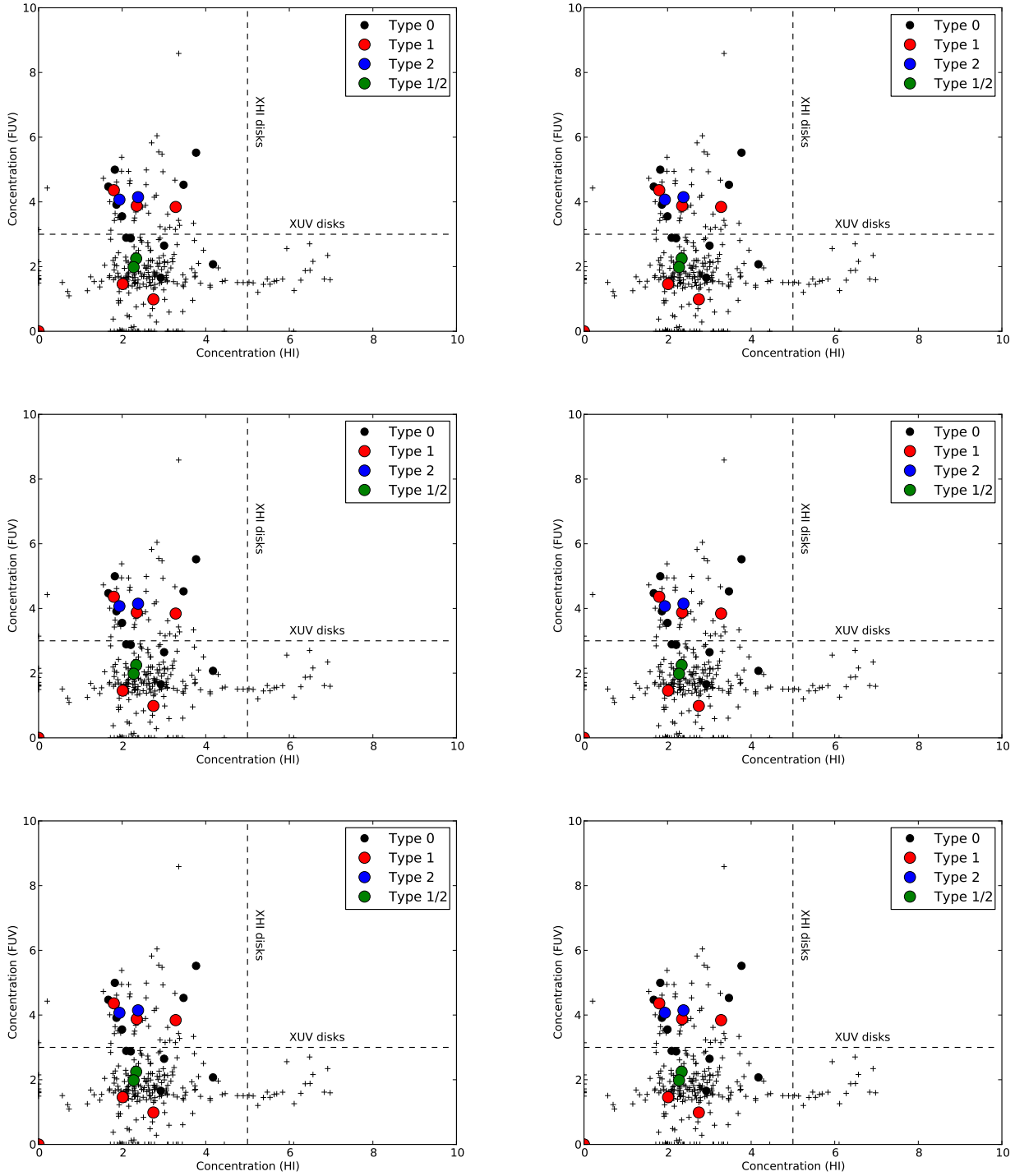


Figure 6. The morphological parameters of the H I disk and FUV data; concentration (C), asymmetry (A), smoothness (S), the Gini index (G), and the second order moment of the brightest 20% of the pixels (M_{20}), and the gini index of the second order moment (G_M).

FUV is promising and we define the following criterion to identify XUV disks in an FUV survey (6'' resolution):

$$|A - (-0.27 \times M_{20} + 0.12)| < 0.14, \quad (7)$$

which works well for the *THINGS* sample and we divide the

linear relation by a factor two for the *WHISP* survey (to account for the $\sim 12''$ resolution):

$$|A - (-0.27 \times M_{20} + 0.12)/2| < 0.14. \quad (8)$$

Both are illustrated in Figure 11 with dashed lines. Table 3 lists the two criteria the simple concentration criterion

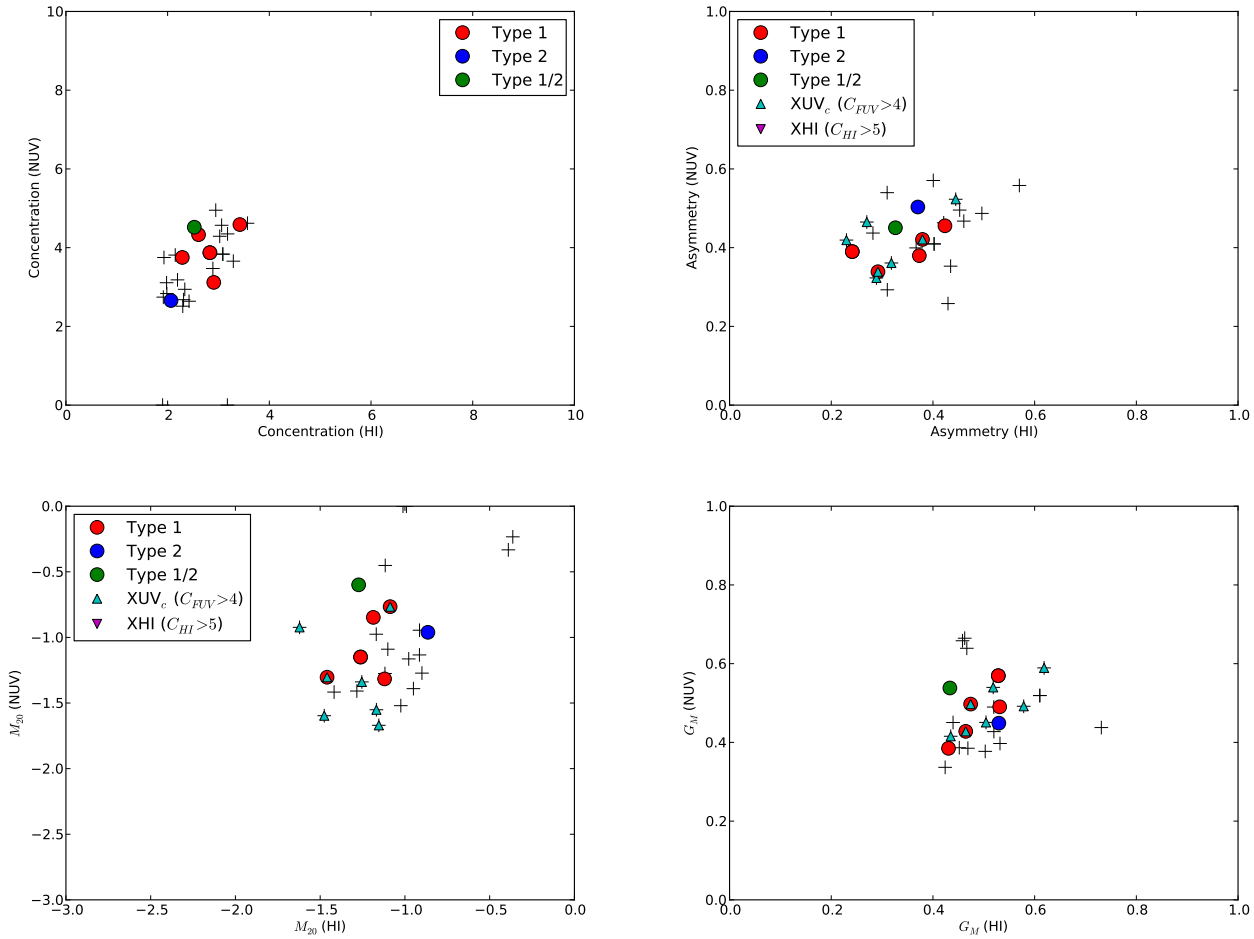


Figure 7. The morphological parameters of the H I disk and NUV for the *THINGS* galaxies with the XUV disk classification from Thilker et al. (2007).

and the M_{20} -Asymmetry one (adjusted for each survey) and their success rate (percentage of all bona-fide XUV disks included) and contamination rate (percentage of all classified objects that are non-XUV). The M_{20} -Asymmetry criterion selects most XUV but with a contamination of some 55% of non-XUV disks. A future search for XUV disks could therefore use this as a first cut before visual classification. Given the 109 *WHISP* galaxies selected by this criterion (Table ??), 61 of these should be bona-fide XUV disks, 23% of our sample of 266.

5.4 Are XUV disks in interacting H I disks?

Figure 12 shows five of the morphological criteria we used or defined in Holwerda et al. (2011a) to identify those disks that are currently undergoing an interaction (see Figure ?? for a similar plot to Figure 5 in Holwerda et al. (2011d) for a direct comparison). We mark those galaxies identified by Thilker et al. (2007) and those identified as extended UV or H I disks by the concentration parameters.

Based on the H I morphologies, the G_M and $C - M_{20}$ criteria, those H I disks that host an XUV disk are not interacting in the majority of cases. In the case of the other

morphological criteria ($A - G$, $A - M_{20}$, $G - M_{20}$), this distinction is not as clear-cut but XUV disks –either selected by Thilker et al or by their concentration– appear to reside in morphologically very typical H I disks.

At the same time, extended H I disks are often interacting. This is in part because of our definition of an interaction is based on concentration but even in the G_M criterion, these are conspicuously separated from the bulk of the H I disks. Typically, the bona-fide XUV disks selected by an H I morphological selection of an ongoing merger appear to be Type 1, consistent with the first impression from Figures 3 - 2. Thus, mergers appear to be one avenue to generate a Type 1 XUV disk.

If we plot these –as a sanity check– for the *THINGS* sample, the XUV disks identified by Thilker et al. (2007) equally appear not to be interacting based on the G_M criterion, but several are based on $G-A$ or $M_{20}-G$ criteria. Several of the non-XUV disks are interactions in $A-M_{20}$. These criteria would need to be adjusted for the higher resolution of the *THINGS* sample (difficult to do without many mergers in the *THINGS* sample, as we noted in Holwerda et al. 2011c).

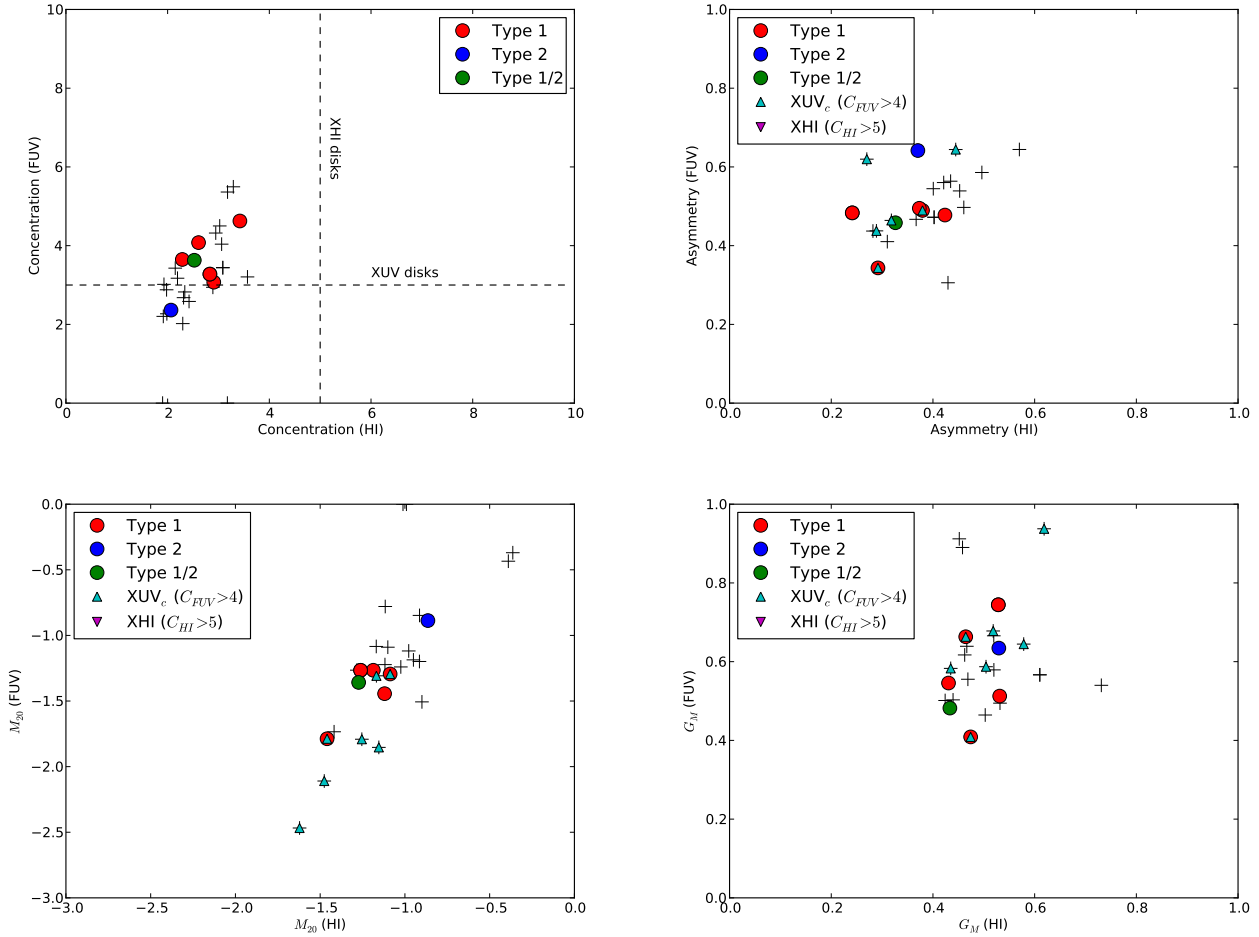


Figure 8. The morphological parameters of the H I disk and FUV for the *THINGS* galaxies with the XUV disk classification from Thilker et al. (2007). Dashed lines are the H I and UV concentration criteria from Figure 6.

6 DISCUSSION

Our first motivation for this study was to explore the possibility if XUV disks could be reliably found using the morphological parameters in UV and H I, especially when computed over a wide aperture such as the H I disk. Based on their morphology parameters in UV and H I, XUV disks identified in Thilker et al. (2007) rarely stand out from the bulk of the *WHISP* sample, with the exception of M_{20} -A and concentration in UV. In the FUV, the M_{20} -A relation appears reasonably successful in identifying XUV disks and the rate in the *WHISP* sample (23%) is consistent with the Thilker et al. (2007) and Lemonias et al. (2011) result, for a survey of late-types such as *WHISP*. The FUV values of Asymmetry and M_{20} could therefore be used to identify candidate XUV disks in the local Universe with GALEX or similar quality UV data or in deep rest-frame UV observations with *HST*. However, these will have to be computed over a much larger area than commonly used (e.g., the de Vaucouleur diameter D_{25} or the Petrosian radius), such as the one defined by the outer H I contour. The quantified H I and UV morphologies do not correlate as closely as they did for the *THINGS* sample in Holwerda et al. (2011c) (their Figure 6). In our opinion, this

is due to the wider range of environments probed by the *WHISP* survey as well as its lower resolution compared to *THINGS*. A closer relation may return for the inner stellar disk and possibly at higher spatial resolution.

Our second motivation for this work on XUV disks was to explore their origin. Are they the (by)product of (a) cold flow accretion, (b) a gravitational interaction or mergers with another galaxy or (c) is photo-dissociation of molecular clouds by the UV regions of the XUV disks responsible for the H I disks?

The fact that the majority of the XUV disks do not reside in morphologically distinct H I disks (Figure 6 and 8), precludes the notion that most XUV disks originate from major interaction between galaxies. Few are selected by the previously defined interaction criteria for H I disks. There are, however, some obvious exceptions (Figure 1). So our naïve interpretation for the origin of Type 1 disks in Figure 1 is only partly supported by H I morphology and only holds for Type 1.

Since extended UV (XUV_c) and extended H I disk (XHI) populations –as defined by their concentration parameter computed over the *same* area– do not coincide (Figure 6, top left panel), a direct link, such as the photo-dissociation

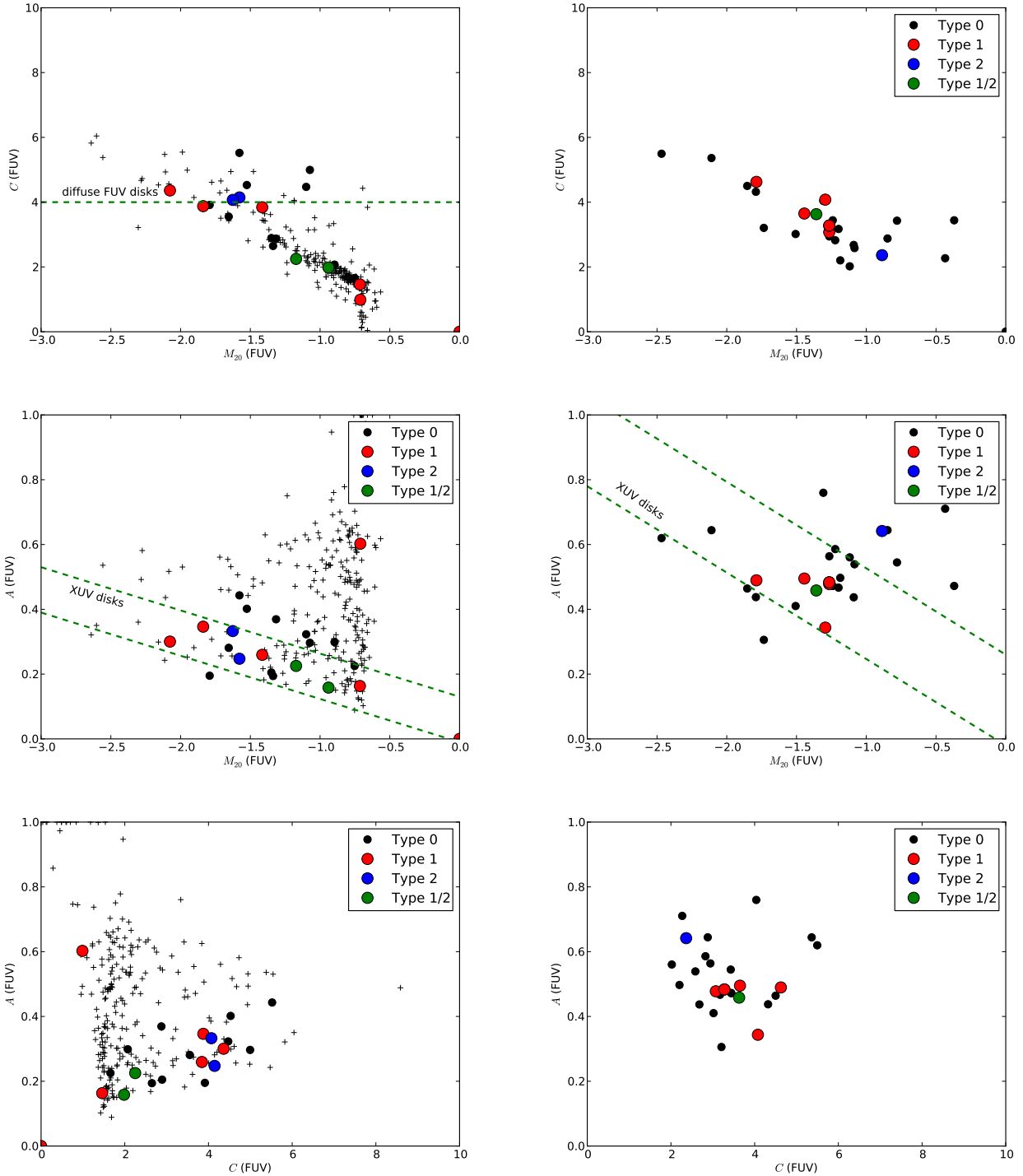


Figure 11. Concentration, Asymmetry and M_{20} in FUV for the *WHISP* (left) and *THINGS* (right) samples with the Thilker et al. classifications marked. $C_{FUV} > 4$ does not select cleanly the XUV disks previously identified by Thilker et al. The M_{20} -Asymmetry criteria (green dashed lines in the middle panels), do select a relatively clean sample of XUV disks from both *WHISP* and *THINGS*.

origin of the H I disk, appears less likely. A closer UV–H I relation in morphology may well still hold within the inner stellar disk, especially since the photo-dissociation scenario was developed to explain the higher column densities of H I in this environment (Allen et al. 1997, 2004; Heiner et al.

2008a,b, 2009, 2010). However, the existence of both the $C_{FUV} > 4$ disks without complementary extended H I disks as well as extended ($C_{HI} > 4$) H I disks without a complementary XUV disk appears to be contradictory to the photo-dissociation origin of XHI disks. Two considerations are still

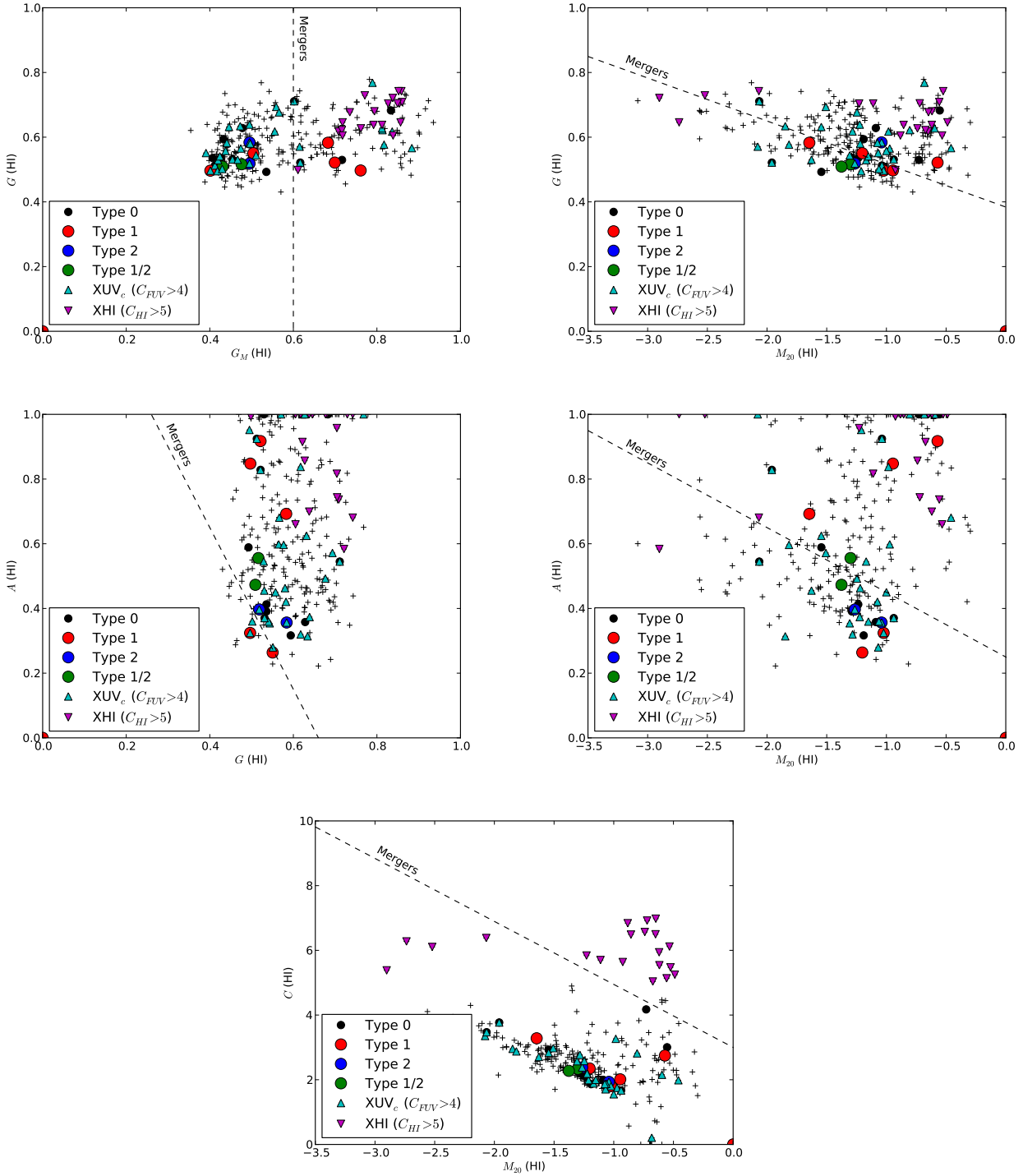


Figure 12. The morphological selection criteria (dashed lines) for H I applied to the *WHISP* sample. Disks are interactions above and to the right of the dashed lines. XUV disks identified either by Thilker et al. or high FUV or H I concentration are marked.

in its favor however, Gogarten et al. (2009) showed that UV emission does not fully trace the lower-level star-formation in the low-column density environments of the outer disk. Thus, the ionizing stars may be lower-mass Main Sequence stars and simply remain undetected in *GALEX* imaging due to their extreme low surface-brightness. And with higher

resolution and more sensitive H I and UV imaging, a closer relation may still return in their quantified morphology (witness the *THINGS* sample). Thus, we cannot completely rule out a photo-dissociation scenario explaining the relation between H I and UV disks. Similarly, Gil de Paz et al. (2007b)

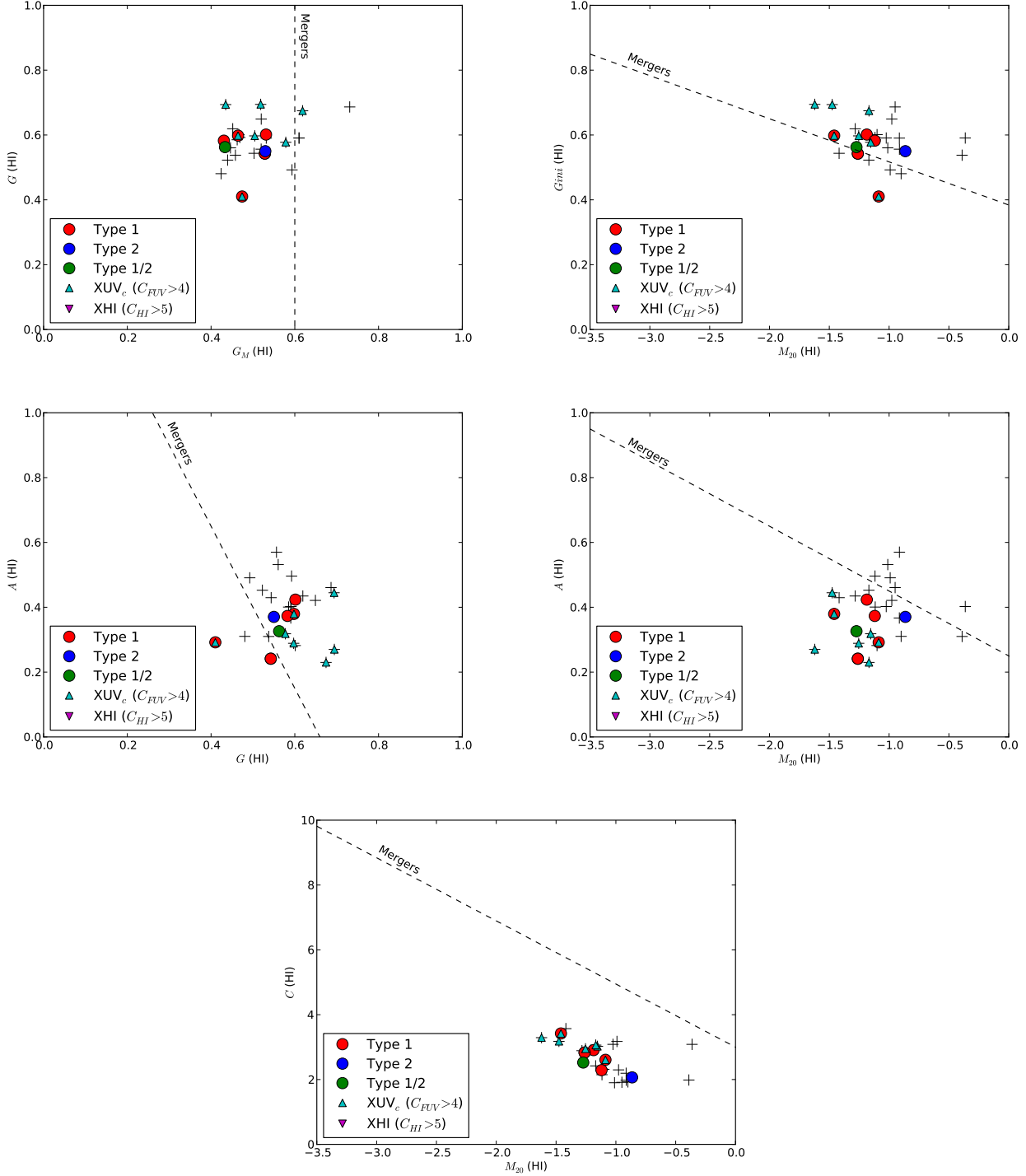


Figure 13. The morphological selection criteria (dashed lines) for H I applied to the *THINGS* sample. XUV disks identified either by Thilker et al. or via their concentration are marked.

find their time-scale argument for a photo-dissociation origin of XUV disks to be inconclusive.

This leaves cold flows as a likely origin for most XUV disks. A number of these Type 1 XUV disks may be the result of a later-stage full merger such as UGC 04862 but judging from the H I morphologies, this is small fraction of

the full XUV or XUV_c sample. Cold flows occur as both a steady trickle along a filament of the Cosmic Web as well as discrete accretion in the form of the cold gas originally associated with a small satellite.

There are indirect signs that cold flows are indeed the most common cause for XUV disks. For example, at least

three of the nine *THINGS* galaxies with an XUV disk (M83, NGC 4736 and NGC 5055) are currently cannibalizing a small companion (Martínez-Delgado et al. 2010). Satellites embedded in the gas filament are one of two fueling mechanisms of cold flow; discrete and trickle cold flows (Kereš et al. 2005). The acquired cold gas accompanying the cannibalized companion is a likely trigger for the formation UV complexes. Similarly, those disks selected by their extended UV emission (Figure ??), often appear to have flocculent, low-column density H I morphologies, which *may* point to recent cold accretion. A few cases (UGC 7081, 7651, and 7853) are obviously interacting major mergers with accompanying H I/UV tidal features. In contrast, the XHI disks are nearly always small galaxies with an obvious close companion (Figure ??), which makes a tidal origin likely for their very extended H I disk.

The quantified morphologies of the *WHISP* H I and UV disks are not conclusive evidence that cold flows are responsible for the XUV complexes but certainly suggest this is the most likely origin for most, with a few exception due to major interactions.

7 CONCLUSIONS

Based on the quantified morphology of the H I and UV maps of the *WHISP* sample of galaxies, we conclude the following:

1. There are distinct galaxy populations that stand out by their high concentration values in FUV or H I (XUV_c and XHI throughout the paper). These population do not overlap. Some known XUV disks are in the XUV_c sample (Figures 6-a 6-e, 8-a and 8-c). To compute this concentration index, the outer H I contour is needed to delineate the extent of the disk.
2. The fact that relative dilute UV disks ($C_{FUV} > 4$) and H I disks ($C_{HI} > 5$) population do not overlap at all and the lack of close morphological relations in any other parameters together suggest that a common small-scale origin for the UV and H I disks, such as a photodissociation of molecular hydrogen scenario, is less likely for XUV disks (but may still very much hold for the inner disks).
3. Asymmetry and M_{20} can be used in combination to select XUV disks with reasonable reliability (80% included) but substantial contamination (55%), when properly calibrated for the survey's spatial resolution (equation 7 and 8) and the morphologies computed over a large enough aperture. With this selection, one can find the number of XUV disks in a survey or candidates for visual classification (Figure 11).
4. Based on the morphology of the H I disk in which they occur, XUV disks appear not to occur often in tidally disturbed gas disks (Figures 12 and 13).
5. In a few cases, the XUV disk *is* the product of a major merger; for example UGC 04862, identified by Thilker et al. (2007) and UGC 7081, 7651, and 7853, identified by their large FUV concentration. This appears to be an avenue to form *some* of the Type 1 XUV disks.
6. The H I morphology and anecdotal evidence for small satellite cannibalism all point to a third mechanism for the origin of most XUV disks; cold flow accretion.

With the emergence of new and refurbished radio observatories in preparation for the future Square Kilometre

Array (SKA; Carilli & Rawlings 2004), a new window on the 21 cm emission line of atomic hydrogen gas (H I) is opening. The two SKA precursors, the South African Karoo Array Telescope (MeerKAT; Booth et al. 2009; Jonas 2007; de Blok et al. 2009), and the Australian SKA Pathfinder (ASKAP; Johnston 2007; Johnston et al. 2007, 2008a,b, 2009) stand poised to observe a large number of Southern Hemisphere galaxies in H I in the nearby Universe ($z < 0.2$). In addition, the Extended Very Large Array (EVLA; Napier 2006) and the APerture Tile In Focus instrument (APERTIF; Verheijen et al. 2008; Oosterloo et al. 2009) on the Westerbork Synthesis Radio Telescope (WSRT) will do the same for the Northern Hemisphere. The surveys conducted with these new and refurbished facilities will add new, high-resolution, H I observations on many thousands of galaxies. In the case of WALLABY (Koribalski et al. *in preparation*), these will be of similar quality spatial resolution as the *WHISP* survey.

Combining these with existing UV observations from GALEX, we can explore the relation between the morphology of the atomic hydrogen and ultraviolet light for much greater samples and in much greater detail. An application of the Asymmetry- M_{20} identification of XUV disks in the GALEX Nearby Galaxy Atlas (Gil de Paz et al. 2007a) or a sample similar to Lemonias et al. (2011) could reveal additional examples but the combination with deep H I observations can prove the link with cold flows for the majority of XUV disks.

ACKNOWLEDGMENTS

The authors would like to thank D. Thilker for discussions at the Cloister See-On conference, the audience at Leiden Observatory for encouragement for this work and the anonymous referee for his or her comments that improved the science and writing of this paper. The authors acknowledge the use of the HyperLeda database <http://leda.univ-lyon1.fr>, the NASA/IPAC Extragalactic Database (NED) which is operated by the Jet Propulsion Laboratory, California Institute of Technology, under contract with the National Aeronautics and Space Administration, and the Westerbork on the Web (WoW) project (<http://www.astron.nl/wow/>).

The Westerbork Synthesis Radio Telescope is operated by the Netherlands Institute for Radio Astronomy AS-TRON, with support of NWO. Based on observations made with the NASA Galaxy Evolution Explorer. GALEX is operated for NASA by the California Institute of Technology under NASA contract NAS5-98034.

REFERENCES

- Alberts S., Calzetti D., Dong H., Johnson L. C., Dale D. A., Bianchi L., Chandar R., Kennicutt R. C., Meurer G. R., Regan M., Thilker D., 2011, ArXiv e-prints
- Allen R. J., 2002, in Astronomical Society of the Pacific Conference Series, Vol. 276, Seeing Through the Dust: The Detection of HI and the Exploration of the ISM in Galaxies, Taylor A. R., Landecker T. L., Willis A. G., eds., p. 288
- Allen R. J., Heaton H. I., Kaufman M. J., 2004, ApJ, 608, 314

- Allen R. J., Knapen J. H., Bohlin R., Stecher T. P., 1997, *ApJ*, 487, 171
- Begeman K. G., 1989, *A&A*, 223, 47
- Bertin E., Arnouts S., 1996, *A&AS*, 117, 393, provided by the NASA Astrophysics Data System
- Bigiel F., Leroy A., Seibert M., Walter F., Blitz L., Thilker D., Madore B., 2010a, *ArXiv e-prints*
- Bigiel F., Leroy A., Walter F., Blitz L., Brinks E., de Blok W. J. G., Madore B., 2010b, *ArXiv e-prints*
- Bigiel F., Leroy A., Walter F., Brinks E., de Blok W. J. G., Madore B., Thornley M. D., 2008, *AJ*, 136, 2846
- Boomsma R., Oosterloo T. A., Fraternali F., van der Hulst J. M., Sancisi R., 2008, *A&A*, 490, 555
- Booth R. S., de Blok W. J. G., Jonas J. L., Fanaroff B., 2009, *ArXiv e-prints/0910.2935*
- Bresolin F., Ryan-Weber E., Kennicutt R. C., Goddard Q., 2009, *ApJ*, 695, 580
- Carilli C. L., Rawlings S., 2004, *New A Rev.*, 48, 979
- Conselice C. J., 2003, *ApJS*, 147, 1
- Cuillandre J., Lequeux J., Allen R. J., Mellier Y., Bertin E., 2001, *ApJ*, 554, 190
- de Blok W. J. G., Jonas J., Fanaroff B., Holwerda B. W., Bouchard A., Blyth S., van der Heyden K., Pirzkal N., 2009, in *Panoramic Radio Astronomy: Wide-field 1-2 GHz Research on Galaxy Evolution*
- Dong H., Calzetti D., Regan M., Thilker D., Bianchi L., Meurer G. R., Walter F., 2008, *AJ*, 136, 479
- Elson E. C., de Blok W. J. G., Kraan-Korteweg R. C., 2011, *ArXiv e-prints*
- Ferguson A. M. N., Wyse R. F. G., Gallagher J. S., Hunter D. A., 1998, *ApJ*, 506, L19
- Gil de Paz A., Boissier S., Madore B. F., Seibert M., Joe Y. H., Boselli A., Wyder T. K., Thilker D., Bianchi L., Rey S.-C., Rich R. M., Barlow T. A., Conrow T., Forster K., Friedman P. G., Martin D. C., Morrissey P., Neff S. G., Schiminovich D., Small T., Donas J., Heckman T. M., Lee Y.-W., Milliard B., Szalay A. S., Yi S., 2007a, *ApJS*, 173, 185
- Gil de Paz A., Madore B. F., Boissier S., Swaters R., Popescu C. C., Tuffs R. J., Sheth K., Kennicutt Jr. R. C., Bianchi L., Thilker D., Martin D. C., 2005, *ApJ*, 627, L29
- Gil de Paz A., Madore B. F., Boissier S., Thilker D., Bianchi L., Sánchez Contreras C., Barlow T. A., Conrow T., Forster K., Friedman P. G., Martin D. C., Morrissey P., Neff S. G., Rich R. M., Schiminovich D., Seibert M., Small T., Donas J., Heckman T. M., Lee Y.-W., Milliard B., Szalay A. S., Wyder T. K., Yi S., 2007b, *ApJ*, 661, 115
- Gogarten S. M., Dalcanton J. J., Williams B. F., Seth A. C., Dolphin A., Weisz D., Skillman E., Holtzman J., Cole A., Girardi L., de Jong R. S., Karachentsev I. D., Olsen K., Rosema K., 2009, *ApJ*, 691, 115
- Heald G., Allan J., Zschaechner L., Kamphuis P., Rand R., Józsa G., Gentile G., 2011a, in *IAU Symposium*, Vol. 277, *IAU Symposium*, C. Carignan, F. Combes, & K. C. Freeman, ed., pp. 59–62
- Heald G., Józsa G., Serra P., Zschaechner L., Rand R., Fraternali F., Oosterloo T., Walterbos R., Jütte E., Gentile G., 2011b, *A&A*, 526, A118
- Heiner J. S., Allen R. J., Emonts B. H. C., van der Kruit P. C., 2008a, *ApJ*, 673, 798
- Heiner J. S., Allen R. J., van der Kruit P. C., 2009, in *The Evolving ISM in the Milky Way and Nearby Galaxies* —, 2010, *ApJ*, 719, 1244
- Heiner J. S., Allen R. J., Wong O. I., van der Kruit P. C., 2008b, *A&A*, 489, 533
- Holwerda B. W., 2005, *astro-ph/0512139*
- Holwerda B. W., Pirzkal N., Cox T. J., de Blok W. J. G., Weniger J., Bouchard A., Blyth S.-L., van der Heyden K. J., 2011a, *MNRAS*, 416, 2426
- Holwerda B. W., Pirzkal N., de Blok W. J. G., Bouchard A., Blyth S.-L., van der Heyden K. J., 2011b, *MNRAS*, 416, 2437
- Holwerda B. W., Pirzkal N., de Blok W. J. G., Bouchard A., Blyth S.-L., van der Heyden K. J., Elson E. C., 2011c, *MNRAS*, 416, 2401
- , 2011d, *MNRAS*, 416, 2415
- Holwerda B. W., Pirzkal N., de Blok W. J. G., van Driel W., 2011e, *MNRAS*, 416, 2447
- Johnston S., 2007, in *From Planets to Dark Energy: the Modern Radio Universe*. October 1-5 2007, The University of Manchester, UK. Published online at SISSA, Proceedings of Science, p.6
- Johnston S., Bailes M., Bartel N., Baugh C., Bietenholz M., Blake C., Braun R., Brown J., Chatterjee S., Darling J., Deller A., Dodson R., Edwards P. G., Ekers R., Ellingsen S., Feain I., Gaensler B. M., Haverkorn M., Hobbs G., Hopkins A., Jackson C., James C., Joncas G., Kaspi V., Kilborn V., Koribalski B., Kothes R., Landecker T. L., Lenc E., Lovell J., Macquart J.-P., Manchester R., Matthews D., McClure-Griffiths N. M., Norris R., Pen U.-L., Phillips C., Power C., Protheroe R., Sadler E., Schmidt B., Stairs I., Staveley-Smith L., Stil J., Taylor R., Tingay S., Tzioumis A., Walker M., Wall J., Wolleben M., 2007, *Publications of the Astronomical Society of Australia*, 24, 174
- Johnston S., Feain I. J., Gupta N., 2009, in *Astronomical Society of the Pacific Conference Series*, Vol. 407, *Astronomical Society of the Pacific Conference Series*, D. J. Saikia, D. A. Green, Y. Gupta, & T. Venturi, ed., pp. 446–+
- Johnston S., Taylor R., Bailes M., Bartel N., Baugh C., Bietenholz M., Blake C., Braun R., Brown J., Chatterjee S., Darling J., Deller A., Dodson R., Edwards P., Ekers R., Ellingsen S., Feain I., Gaensler B., Haverkorn M., Hobbs G., Hopkins A., Jackson C., James C., Joncas G., Kaspi V., Kilborn V., Koribalski B., Kothes R., Landecker T., Lenc A., Lovell J., Macquart J.-P., Manchester R., Matthews D., McClure-Griffiths N., Norris R., Pen U.-L., Phillips C., Power C., Protheroe R., Sadler E., Schmidt B., Stairs I., Staveley-Smith L., Stil J., Tingay S., Tzioumis A., Walker M., Wall J., Wolleben M., 2008a, *Experimental Astronomy*, 22, 151
- , 2008b, *Experimental Astronomy*, 22, 151
- Jonas J., 2007, in *From Planets to Dark Energy: the Modern Radio Universe*. October 1-5 2007, The University of Manchester, UK. Published online at SISSA, Proceedings of Science, p.7
- Kennicutt Jr. R. C., 1998, *ApJ*, 498, 541
- Kereš D., Katz N., Weinberg D. H., Davé R., 2005, *MNRAS*, 363, 2
- Kleinmann S. G., Lysaght M. G., Pughe W. L., Schneider S. E., Skrutskie M. F., Weinberg M. D., Price S. D., Matthews K. Y., Soifer B. T., Huchra J. P., 1994, *Exp.*

- Astronomy, 3, 65
- Lelièvre M., Roy J.-R., 2000, *AJ*, 120, 1306
- Lemonias J. J., Schiminovich D., Thilker D., Wyder T. K., Martin D. C., Seibert M., Treyer M. A., Bianchi L., Heckman T. M., Madore B. F., Rich R. M., 2011, *ArXiv e-prints*
- Lotz J. M., Primack J., Madau P., 2004, *AJ*, 128, 163
- Martin D. C., Fanson J., Schiminovich D., Morrissey P., Friedman P. G., Barlow T. A., Conrow T., Grange R., Jelinsky P. N., Milliard B., Siegmund O. H. W., Bianchi L., Byun Y.-I., Donas J., Forster K., Heckman T. M., Lee Y.-W., Madore B. F., Malina R. F., Neff S. G., Rich R. M., Small T., Surber F., Szalay A. S., Welsh B., Wyder T. K., 2005, *ApJ*, 619, L1
- Martínez-Delgado D., Gabany R. J., Crawford K., Zibetti S., Majewski S. R., Rix H.-W., Fliri J., Carballo-Bello J. A., Bardalez-Gagliuffi D. C., Peñarrubia J., Chonis T. S., Madore B., Trujillo I., Schirmer M., McDavid D. A., 2010, *AJ*, 140, 962
- Meurer G. R., Carignan C., Beaulieu S. F., Freeman K. C., 1996, *AJ*, 111, 1551
- Meurer G. R., Staveley-Smith L., Killeen N. E. B., 1998, *MNRAS*, 300, 705
- Meurer G. R., Wong O. I., Kim J. H., Hanish D. J., Heckman T. M., Werk J., Bland-Hawthorn J., Dopita M. A., Zwaan M. A., Koribalski B., Seibert M., Thilker D. A., Ferguson H. C., Webster R. L., Putman M. E., Knezek P. M., Doyle M. T., Drinkwater M. J., Hoopes C. G., Kilborn V. A., Meyer M., Ryan-Weber E. V., Smith R. C., Staveley-Smith L., 2009, *ApJ*, 695, 765
- Moffett A. J., Kannappan S. J., Baker A. J., Laine S., 2011, *ArXiv e-prints*
- Muñoz-Mateos J. C., Gil de Paz A., Zamorano J., Boissier S., Dale D. A., Pérez-González P. G., Gallego J., Madore B. F., Bendo G., Boselli A., Buat V., Calzetti D., Moustakas J., Kennicutt R. C., 2009, *ApJ*, 703, 1569
- Napier P. J., 2006, in *Astronomical Society of the Pacific Conference Series*, Vol. 356, *Revealing the Molecular Universe: One Antenna is Never Enough*, D. C. Backer, J. M. Moran, & J. L. Turner, ed., pp. 65–+
- Nilson P., 1973, *Uppsala general catalogue of galaxies. Acta Universitatis Upsaliensis. Nova Acta Regiae Societatis Scientiarum Upsaliensis - Uppsala Astronomiska Observatoriums Annaler*, Uppsala: Astronomiska Observatorium, 1973
- Noordermeer E., van der Hulst J. M., Sancisi R., Swaters R. A., van Albada T. S., 2005a, *A&A*, 442, 137
- , 2005b, *A&A*, 442, 137
- Oosterloo T., Verheijen M., van Cappellen W., Bakker L., Heald G., Ivashina M., 2009, *ArXiv e-prints*
- Roškar R., Debattista V. P., Brooks A. M., Quinn T. R., Brook C. B., Governato F., Dalcanton J. J., Wadsley J., 2010, *MNRAS*, 408, 783
- Sancisi R., Fraternali F., Oosterloo T., van der Hulst T., 2008, *A&A Rev.*, 15, 189
- Scarlata C., Carollo C. M., Lilly S., Sargent M. T., Feldmann R., Kampczyk P., Porciani C., Koekemoer A., Scoville N., Kneib J.-P., Leauthaud A., Massey R., Rhodes J., Tasca L., Capak P., Maier C., McCracken H. J., Mobasher B., Renzini A., Taniguchi Y., Thompson D., Sheth K., Ajiki M., Aussel H., Murayama T., Sanders D. B., Sasaki S., Shioya Y., Takahashi M., 2007, *ApJS*, 172, 406
- Swaters R. A., Balcells M., 2002, *A&A*, 390, 863
- Swaters R. A., van Albada T. S., van der Hulst J. M., Sancisi R., 2002a, *A&A*, 390, 829
- , 2002b, *A&A*, 390, 829
- Thilker D. A., Bianchi L., Boissier S., Gil de Paz A., Madore B. F., Martin D. C., Meurer G. R., Neff S. G., Rich R. M., Schiminovich D., Seibert M., Wyder T. K., Barlow T. A., Byun Y.-I., Donas J., Forster K., Friedman P. G., Heckman T. M., Jelinsky P. N., Lee Y.-W., Malina R. F., Milliard B., Morrissey P., Siegmund O. H. W., Small T., Szalay A. S., Welsh B. Y., 2005a, *ApJ*, 619, L79
- Thilker D. A., Bianchi L., Meurer G., Gil de Paz A., Boissier S., Madore B. F., Boselli A., Ferguson A. M. N., Muñoz-Mateos J. C., Madsen G. J., Hameed S., Overzier R. A., Forster K., Friedman P. G., Martin D. C., Morrissey P., Neff S. G., Schiminovich D., Seibert M., Small T., Wyder T. K., Donas J., Heckman T. M., Lee Y.-W., Milliard B., Rich R. M., Szalay A. S., Welsh B. Y., Yi S. K., 2007, *ApJS*, 173, 538
- Thilker D. A., Hoopes C. G., Bianchi L., Boissier S., Rich R. M., Seibert M., Friedman P. G., Rey S.-C., Buat V., Barlow T. A., Byun Y.-I., Donas J., Forster K., Heckman T. M., Jelinsky P. N., Lee Y.-W., Madore B. F., Malina R. F., Martin D. C., Milliard B., Morrissey P. F., Neff S. G., Schiminovich D., Siegmund O. H. W., Small T., Szalay A. S., Welsh B. Y., Wyder T. K., 2005b, *ApJ*, 619, L67
- Torres-Flores S., Mendes de Oliveira C., de Mello D. F., Scarano Jr S., Urrutia-Viscarra F., 2012, *ArXiv e-prints*
- van der Hulst J. M., 2002, in *Astronomical Society of the Pacific Conference Series*, Vol. 276, *Seeing Through the Dust: The Detection of HI and the Exploration of the ISM in Galaxies*, Taylor A. R., Landecker T. L., Willis A. G., eds., pp. 84–+
- van der Hulst J. M., van Albada T. S., Sancisi R., 2001, in *Astronomical Society of the Pacific Conference Series*, Vol. 240, *Gas and Galaxy Evolution*, Hibbard J. E., Rupen M., van Gorkom J. H., eds., pp. 451–+
- Verheijen M. A. W., Oosterloo T. A., van Cappellen W. A., Bakker L., Ivashina M. V., van der Hulst J. M., 2008, in *American Institute of Physics Conference Series*, Vol. 1035, *The Evolution of Galaxies Through the Neutral Hydrogen Window*, R. Minchin & E. Momjian, ed., pp. 265–271
- Walter F., Brinks E., de Blok W. J. G., Bigiel F., Kennicutt R. C., Thornley M. D., Leroy A., 2008, *AJ*, 136, 2563
- Werk J. K., Putman M. E., Meurer G. R., Thilker D. A., Allen R. J., Bland-Hawthorn J., Kravtsov A., Freeman K., 2010, *ApJ*, 715, 656
- Zaritsky D., Christlein D., 2007, *AJ*, 134, 135
- Zschaechner L. K., Rand R. J., Heald G. H., Gentile G., Kamphuis P., 2011, *ApJ*, 740, 35
- Zwaan M. A., van der Hulst J. M., Briggs F. H., Verheijen M. A. W., Ryan-Weber E. V., 2005, *MNRAS*, 364, 1467